arXiv:cond-mat/0304389v1 [cond-mat.mes-hall] 17 Apr 2003

Transition from tunneling to direct contact in tungsten nanojunctions

A. Halbritter, Sz. Csonka and G. Mihály
Department of Physics, Institute of Physics, Budapest University of Technology and Economics, 1111 Budapest, Hungary

E. Jurdik, O.Yu. Kolesnychenko, O.I. Shklyarevskii†, S. Speller and H. van Kempen
NSRIM, University of Nijmegen, Toernooiveld 1, 6525 ED Nijmegen, the Netherlands

We apply the mechanically controllable break junctions technique to investigate the transition from tunneling to direct contact in tungsten. This transition is quite different from that of other metals and is determined by the local electronic properties of the tungsten surface and the relief of the electrodes at the point of their closest proximity. The conductance traces show a rich variety of patterns from the avalanche-like jump to a mesoscopic contact to the completely smooth transition between direct contact and tunneling. Due to the occasional absence of an adhesive jump the conductance of the contact can be continuously monitored at ultra-small electrode separations. The conductance histograms of tungsten are either featureless or show two distinct peaks related to the sequential opening of spatially separated groups of conductance channels. The role of surface states of tungsten and their contribution to the junction conductance at sub-Ångstrom electrode separations are discussed.

I. INTRODUCTION

The study of transition from tunneling to direct contact and electrical transport through atomic-sized metallic conductors has been the object of great attention during the last decade. Different types of phenomena, related to both the quantum character of transport and the atomic discreteness of the contact, were observed in 3D nanoconstrictions produced by scanning tunneling microscopes (STM) or mechanically controllable break junctions (MCBJ) [1]. In particular, conductance measurements of breaking nanowires demonstrated a steplike structure of conductance versus electrode separation traces $G(z)$. For single-valence s-metals conductance plateaus are close to the integer multiples of the quantum conductance unit $G_0 = 2e^2/h$. However, simultaneous measurements of both the force and the conductance for breaking gold nanowires demonstrated that jumps between plateaus in the conductance staircase are always correlated with relaxations of the mechanical force and, therefore, with atomic rearrangements in the nanoconstriction [2]. Individual conductance curves $G(z)$ are inherently irreproducible due to the different dynamical evolution of the connective necks during the break. Therefore, analysis of experimental data includes construction of conductance histograms based on a large number of conductance traces. Peaks in the conductance histograms are related to the statistically more probable atomic configurations in the connective neck between the electrodes [3]. For polyvalent metals the main (and sometimes the only) feature in the conductance histograms is a peak corresponding to one-atom point contact [4]. The conductance through such a contact is determined by a few conductance channels intimately related to atomic orbitals [5]. Transition from tunneling to single-atom contact occurs in an avalanche-like way at an electrode separation of ~ 1.5 Å due to the metallic adhesion forces [6]. This sudden jump in conductance precluded measurements of $G(z)$ at sub-Ångstrom distances between the electrodes for all metals studied to date.

While measuring thermal expansion of MCBJ electrodes for different materials, we took notice of the unusually high stability of tungsten tunnel junctions at very close electrode separations [7]. In another study, transmission and scanning electron microscopy images showed no evidence of connective neck formation between tungsten wires [8]. Moreover, measurements of adhesive forces between an atomically-defined W(111) trimer tip and a Au(111) sample revealed no spontaneous jump to contact [9]. These unusual properties of tungsten nanocontacts motivated us to carry out further extensive investigations.

In this paper we present our experiments with tungsten MCBJ. Our aim was to examine the behavior of tungsten nanojunctions during the transition between tunneling and direct contact and to what extent this behavior is influenced by the unique mechanical and electronic properties of tungsten. We show that very often the adhesive jumps of conductance are absent and that the transition to single atom contact is smooth. This permitted us to investigate the junction at ultra-small electrode separations. By employing the conductance histogram technique we determined the preferential values of conductance during the fracture of the junction to be about 1 G_0 and 2 G_0. Also, we measured the conductance histograms of tantalum and molybdenum (as two nearest neighbors of tungsten in the periodic table of elements) to provide additional support for our interpretation.

II. EXPERIMENTAL SETUP

We employed the traditional MCBJ technique, described elsewhere [1], with a modified sample mounting (Fig. 1). This mounting includes two $6 \times 2.5 \times 1$ mm pieces of shear piezo-ceramic (which gives horizontal displacement of its surface when voltage is applied) glued at

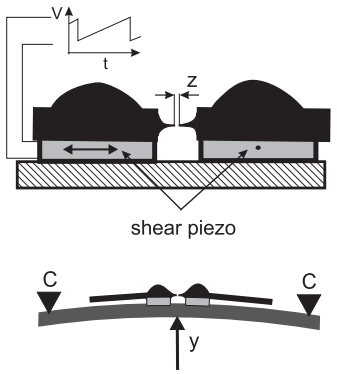

FIG. 1: Modified sample mounting. The tungsten wire is glued on top of shear piezo-ceramic attached to a phosphor bronze bending beam. The distance between the electrodes is controlled by vertically pushing the bending beam at the middle or by applying voltage on the left-hand side shear piezo. All distances are exaggerated for clarity.

the center of a phosphor bronze bending beam. A polycrystalline tungsten wire with a diameter of 100 μm was attached to the top of the piezo's with two small drops of hard epoxy (Stycast 850FT). The central section of the wire was then electrochemically etched in a 25% solution of KOH down to 5–10 μm at its thinnest part. The wire was broken at 4.2 K in an ultra-high vacuum environment by bending the beam. The distance between the electrodes was fine tuned by changing the deflection of the bending beam or applying voltage to the left-hand side shear piezo. The relative displacement of the electrodes was calibrated using the exponential part of $G(z)$ traces in the tunneling regime (assuming a work function for tungsten $\phi \simeq 4.5$ eV) as well as by measuring field emission resonance spectra [10]. The contact conductance was measured using a current-to-voltage converter with a gain of 0.1 V/μA. Conductance versus electrode separation traces $G(z)$ were measured in a slow mode (2–30 points/s) using Keithley 2182 nanovoltmeters in order to cover over 7 orders of magnitude in the conductance during transition from tunneling to direct contact. Conductance traces for building conductance histograms were recorded with an AT-MIO-16XE-50 National Instruments data acquisition board (sampling rate of 20000 points/s and resolution of 16 bits). During this acquisition a ramp voltage with a frequency of 5–50 Hz was applied to the shear piezo to establish a repeated fracture of the junction.

The sample surfaces were characterized by scanning the electrodes with the two shear piezo's in the constant current mode. We found atomically flat parts up to 5–10 nm in length alternating with irregularities of 5–15 Å in height. It should be noted that these STM-like measurements with two "blunt" electrodes are rather qualitative and the numbers presented are only rough estimates.

We analyzed thoroughly more than 200 conductance histograms measured for 12 different samples.

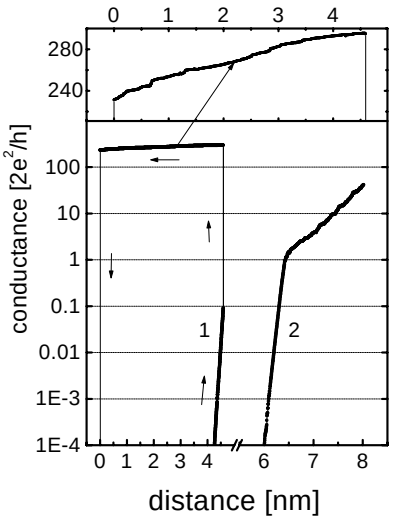

FIG. 2: Two extreme cases of $G(z)$ traces for W MCBJ. 1 – avalanche-like transition from tunneling to a low-ohmic contact. The upper panel shows the contact conductance in the process of retraction. 2 – transition from tunneling to direct contact without spontaneous formation of an adhesive neck.

III. RESULTS

We investigated the transition from the tunneling regime to direct contact for tungsten MCBJ by performing conductance measurements during slow, continuous approach or retraction of the electrodes. These measurements revealed a rich variety of $G(z)$ traces. All of them fall between two extreme cases shown in Fig. 2. Curve 1 demonstrates an avalanche-like transition from $G \approx 0.01$–$0.1\ G_0$ to 100–1000 G_0. This indicates the formation of a mesoscopic contact with a cross-section of 10–100 nm^2 between two flat portions of the electrodes. Subsequent retraction of the electrodes produced only small changes in the contact conductance over a retreat distance of $\gtrsim 4$ nm, which were followed by sudden disconnection (upper panel in Fig. 2). During 5–10 minutes after disconnection, the distance between the electrodes increased as deduced from the transient decrease of the measured tunnel current. After the full relaxation of the sample, the original curve could be reproduced accurately, indicating that no irreversible changes of the electrode relief occurred. The other extreme case – curve 2 in Fig. 2 – demonstrates a smooth transition from tunneling to direct contact with no sign of spontaneous formation of an adhesive neck. The majority of $G(z)$ curves exhibited combination of smooth changes of the conductance and sudden jumps with amplitudes ranging from $0.1G_0$ up to few G_0.

We also performed statistical analysis of conductance traces by employing the conductance histogram technique. We found that tungsten nanojunctions have a particular tendency to show reproducible, almost identical conductance traces when indentation of the electrodes

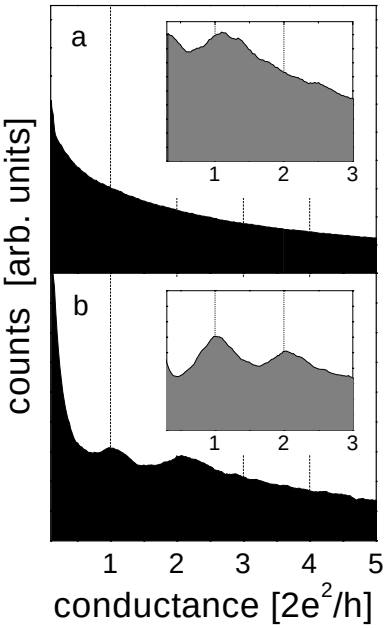

FIG. 3: Conductance histograms for W MCBJ based on 10000 $G(z)$ traces. (a) – featureless histogram. (b) – histogram with peaks close to integers of $2e^2/h$. Insets in (a) and (b): histograms for the corresponding data sets after filtering out the featureless curves.

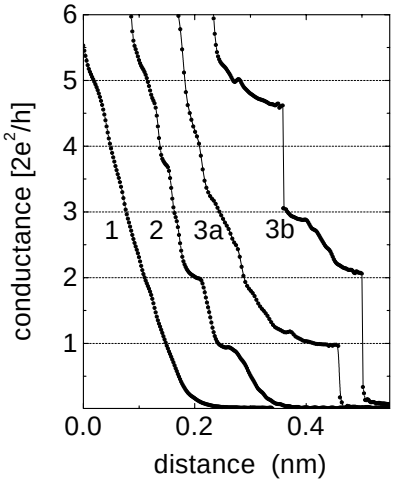

FIG. 4: Typical conductance traces for W. Curve 1 – featureless curve. Curve 2 – smooth transition to tunneling with distinct plateaus. Curves 3a and 3b – traces with sudden jumps of conductance.

is not sufficient. If proper care is taken and in every cycle contacts of $G \gtrsim 30$–$40\ G_0$ are formed, the break occurs in a large variety of ways. In this latter case a statistical approach to data analysis is justified. In sharp contrast to other metals, the conductance histograms of tungsten do not necessarily exhibit the same pattern when the contact site is shifted by the right-hand side shear piezo or when the sample is replaced. A major part of histograms demonstrated no distinctive features [Fig. 3(a)]. However, on many occasions the histograms showed two peaks at respectively 1–1.2 and 2–2.2 G_0 [Fig. 3(b)], or only one of those two.

In Fig. 4 four characteristic conductance traces are presented. Curve 1 shows a smooth and completely featureless transition from direct contact to tunneling. For a tungsten junction this kind of transition is frequently present and gives rise to the featureless background in the conductance histograms. This background is suppressed when these featureless curves are rejected from the data set by employing a computer filtering algorithm [11]. Then, either peaks invisible in the original histogram appear [inset in Fig. 3(a)] or the contrast of peaks is significantly improved [inset in Fig. 3(b)]. Peaks in the histogram naturally arise from conductance traces with distinct features – plateaus – at about $1G_0$ and/or $2G_0$ as demonstrated by curves 2, 3a and 3b in Fig. 4. While curve 2 shows a smooth transition with no jumps, in the case of curves 3a and 3b clear jumps occur near $1G_0$ and $2G_0$, respectively. We note here that conductance traces like those represented by curve 2 are unique to tungsten and were not observed in other metallic contacts.

In our previous analysis we used an algorithm to select the traces with long plateaus [11]. However, it is also important to differentiate between the smooth curves and those with sudden jumps. For this reason every trace was characterized by the largest jump between neighboring data points in the conductance interval $G/G_0 \in [0.3, 3.3]$. By combining these two approaches the traces were classified into the three categories presented in Fig. 4. Using the data set for histogram in Fig 3(b) we found that $\sim 30\%$ of traces exhibited a smooth and featureless transition and roughly 10% of curves show plateaus without sudden jumps. In the rest of the traces clear conductance jumps were found. In order to quantify at which conductance values conductance jumps with $\Delta G_{max} \geq 0.7G_0$ are most likely to occur, we also built up histograms for the position of these sudden transitions. The peaks in the so-built histogram presented in Fig. 5 clearly demonstrate that large conductance jumps are most probable at $G \simeq 1G_0$ and $2G_0$. We emphasize that the relative occurrence of the three different types of conductance traces is sample and site-dependent, and in certain data sets only traces with smooth transitions were present.

IV. DISCUSSION

Our experimental results for tungsten nanojunctions strikingly differ from those obtained for other metals studied so far, that exhibit conductance traces always falling into the same (material-specific) pattern. Especially, the adhesive jump to contact or the tensile overstretching followed by sudden disruption have respectively been found to be an unavoidable attendant of contact formation or breakage. This has precluded measurements of conductance at small electrode separations.

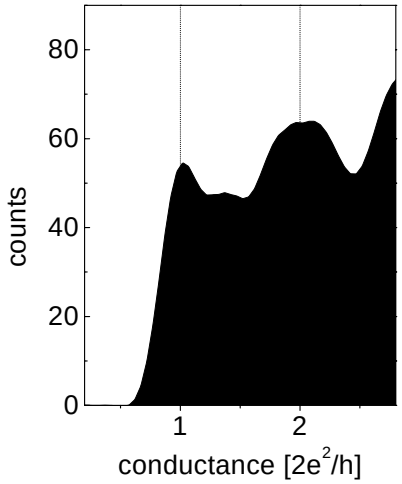

FIG. 5: Histogram for conductance values at which jumps with amplitude $\Delta G > 0.7G_0$ occur.

The occasional absence of these processes is unique for tungsten junctions and we attribute it to the specific mechanical properties of this metal. In particular, this odd junction stability at ultra-small electrode separations permitted us to study the previously unaccessible regime of nanocontact conductance.

The adhesive jump is governed by the the competition between the adhesive and tensile forces [12]. The tensile forces are determined by the stiffness of the electrodes, which is composed from the stiffness of the nanoscale junction itself and the stiffness of the whole setup. The latter can have significant importance in an atomic force microscope with a soft cantilever, however it is not expected to play any role in an MCBJ due to the rigid sample mounting. The stiffness of the junction depends on the strength of the bonds in the material, but also the junction geometry and the crystallographic orientation of the electrodes have a crucial influence on it. Contacts with large opening angle have large stiffness, while in contacts with small opening angle a large amount of layers are involved in the elastic deformation and thus the stiffness is reduced. The stiffness is also reduced, if the contact surfaces are not perpendicular to the contact axis. Then, the electrodes can bend like a cantilever and the elastic behavior is defined by the smaller shear forces.

The elastic behavior of the material is basically determined by the strength of the bonds between the atoms, therefore it is similar at any length-scale and atomic scale systems are well described by bulk elastic constants [2]. The bulk elastic modulus of tungsten ($E_{\mathrm{W}} = 411\,\mathrm{GPa}$) is outstandingly large among all metals. (As a comparison the Youngs modulus of Au, Pt, and Nb is $E_{\mathrm{Au}} = 78\,\mathrm{GPa}$, $E_{\mathrm{Pt}} = 168\,\mathrm{GPa}$, and $E_{\mathrm{Nb}} = 105\,\mathrm{GPa}$, respectively.) On the other hand, the junction geometry is not controllable in MCBJ experiments. In previously studied metals the conductance traces imply that the junction breaks through the process of rupture. In this case the contact geometry is "self-organized" during the neck pulling, so the conditions for the adhesive jumps are similar during each disconnection. Our measurements imply that tungsten breaks in a more brittle way and a large variety of contact geometries are established during the fractures. This, together with the outstanding elastic modulus of tungsten can explain our observations. In "stiff" contact geometries the elastic forces can overcome the adhesion and thereby enable a smooth transition between tunneling and direct contact, while in softer contact geometries the adhesive jumps are still present.

Our interpretation can be tested by comparing the mechanical behavior during the break of further metals with different elastic modulus. For this reason we performed measurements on two neighbors of tungsten in the periodic system, molybdenum and tantalum. These metals have similar electronic properties to tungsten. The elastic modulus of molybdenum is relatively large ($E_{\mathrm{Mo}} = 329\,\mathrm{GPa}$), while tantalum is much softer ($E_{\mathrm{Ta}} = 186\,\mathrm{GPa}$). In agreement with that we found that tantalum always breaks in a jump-like way, while in molybdenum a part of the conductance traces showed a smooth transition.

To explain the avalanche-like motion of hundreds to thousands of atoms in the extreme case presented in Fig. 2 as curve 1, we consider the following three possibilities. The first one corresponds to the motion of a number of atomic layers in the direction normal to the electrode surfaces as assumed in the calculations by Taylor *et al.* [12]. This possibility would require an avalanche of a macroscopic amount of metal. Such a situation can take place only for contacts that act as a very soft spring and thus we do not consider it as the most likely explanation. The second possibility, that would result in the same behavior of the contact conductance, is the transition to direct contact due to bending of the electrodes. This arrangement is likely to occur when flat parts of the electrode surfaces are not perpendicular to the electrode axis. Then, the component of the adhesive force that is normal to the electrode axis causes bending. During our experiments, we observed anomalously high sensitivity of the tungsten MCBJ to acoustic vibrations, such as human voice, that suggests a transverse, spring-like motion of the electrodes. This observation is in favor of the "bending model." As the last possibility, the contact between the electrodes may emerge as a result of dislocation glide or homogeneous shear motion of one of the electrodes [1]. However, in this case it is not possible to explain the reversible behavior of contact conductance through many formation-breaking cycles.

The smooth conductance traces with plateaus at the first two conductance quanta (e.g., curve 2 in Fig. 4) are very close to those expected for conductance quantization in short constrictions [14]. In spite of its attractiveness, we discarded this effect as the possible origin of the peaks in our histograms. Extremely small distances between the plateaus in conductance traces of tungsten, $\Delta z \simeq 30$ pm, suggest a constriction with an opening angle close to 90 degrees (an orifice). In this case the conductance

quantization must be completely suppressed [14]. The shape of these traces is better explained by the sequential closing of conduction channels due to different spatial distribution of the involved electronic states.

For transition d-metals five conductance channels are expected to contribute to the conductance of a single-atom contact according to the number of valence orbitals. The transmission values of these conductance channels were extensively studied for single-atom niobium junctions by tight binding calculations [5] and by measuring subgap structure in the superconducting state [15]. The calculations performed for a simplified one-atom contact geometry revealed a single dominant channel (as a result of the hybridization between the s and d_{z^2} orbitals), two medium-sized channels and two smaller channels that yield together a net conductance of $G = 2$–$3\ G_0$. Both the conductance and the transmission coefficients showed a good agreement with the values determined from the experiment. Such a detailed investigation of the transmission eigenvalues is not available for the rest of the d-metals, and therefore the conduction properties of monoatomic contacts can only be deduced from the conductance histograms. For all non-magnetic transition metals studied so far (Nb, V, Rh, Pd, Ir, Pt) the histograms show a single well-defined peak centered in the region of $G = 1.5$–$2.5\ G_0$, that is attributed to the conductance through a single-atom contact [1, 4]. To date, theoretical calculations have not been performed for the conductance of a single-atom tungsten contact, but its value is presumably in the same range of $G \simeq 1.5$–$2.5\ G_0$.

In tungsten the first peak in the histogram is situated at $1\ G_0$, which is too low to be attributed to a single atom contact with all the channels open. Therefore, rather the second peak at $2\ G_0$ is interpreted as the conductance of a monoatomic contact geometry, where the center atom is closely bound to both electrodes. The peak at $1\ G_0$ is assumably connected to an arrangement where the electrodes are so much separated that only a part of the electronic states have noticeable overlap.

It is well known from STM studies that tungsten surfaces have long protruding surface modes, which have a crucial role in achieving atomic resolution. First principle calculations for the W(001) surface demonstrated that the tunnel current is primarily generated by the $5d_{z^2}$ dangling-bond surface states [16, 17]. At distances > 2 Å from the nuclei the charge density of the surface state is much higher than that of the atomic $6s$-state [18] and so the surface states play a key role in the electron transport at small separations. The conductance through a single channel formed by such surface states can be a good candidate for explaining the conductance plateaus at $1\ G_0$.

The occasional absence of adhesive jump enables us to monitor the transition between the two situations. However, the sequential closing of conductance channels – like curve 2 in Fig. 4 – may only occur for specific electrode configurations, which explains the relatively low percentage of this type of conductance traces.

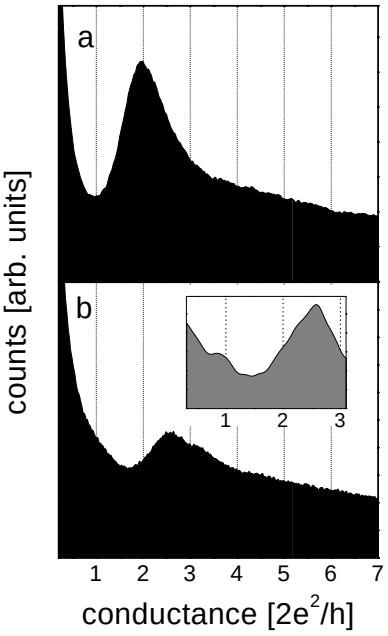

FIG. 6: Conductance histograms for tantalum (a) and molybdenum (b) based on 20000 conductance traces. Inset in (b) shows a histogram for selected 10% of the curves, exhibiting plateaus around $1G_0$.

The conductance histograms of tantalum and molybdenum were also studied. These two neighbors of tungsten in the periodic system have very similar electronic structure to W. Both for Ta and Mo the histograms show a single, well-defined peak situated around $2\ G_0$ and $2.5\ G_0$, respectively (see Fig. 6). This gives further support to the assumption that the conductance through a single atom contact is in the range of $2\ G_0$ for tungsten as well. Though the electronic properties of Mo surfaces are similar to tungsten [20] the histograms show no indication for a peak at $1\ G_0$. In some occasions the computer filtering of the original data set reveals conductance traces with plateaus close to the conductance quantum, and accordingly a small peak around $1\ G_0$ is recovered in the histogram (see inset in Fig. 6(b)).

V. CONCLUSIONS

In conclusion, our measurements have shown that the evolution of conductance during the break of tungsten nanojunctions essentially differs from the ususal behavior of metallic contacts. Due to the large elastic modulus of W and the the non-ductile contact fracture, the adhesive jumps in the conductance traces are occasionally absent. Thank to these completely smooth transitions from direct contact to tunneling, the closing of conductance channels can be continuously monitored at ultra small electrode separations. The study of conductance histograms has shown, that the preferential val-

ues of conductance in tungsten junctions are $1\,G_0$ and $2\,G_0$. The smooth conductance traces with plateaus at these two values are explained by the sequential closing of conductance channels due to their different spatial distribution. The conduction through the long-protruding surface states of tungsten might be responsible for the plateaus at $1\,G_0$.

The limitations of MCBJ technique precluded us from drawing a more exact and persuasive conclusion. The current data can greatly be improved by simultaneous measurements of the conductance and the forces in the course of electrode approach for contacts with a well-defined tip/sample shape and orientation. To our opinion, the details of the process of avalanche-like transition to direct contact and subsequent break can be visualized with a high resolution transmission electron microscope operating in UHV.

Acknowledgments

The authors are grateful to A.J. Toonen, J. Hermsen and J. Gerritsen for invaluable technical assistance. Part of this work was supported by the Stichting voor Fundamenteel Onderzoek der Materie (FOM) which is financially supported by the Nederlandse Organisatie voor Wetenschappelijk Onderzoek (NWO). The Hungarian Research Funds OTKA TO37451, TS040878, N31769 and a NWO grant for Dutch-Hungarian cooperation are also acknowledged. O.I.S. wishes to thank the NWO for a visitor's grant.

---

† Also at: B. Verkin Institute for Low Temperature Physics & Engineering, National Academy of Science of Ukraine, 47 Lenin Av., 61164, Kharkov, Ukraine.

[1] J.M. van Ruitenbeek, in "Metal Cluster on Surfaces: Structure, Quantum Properties, Physical Chemistry"' K.H. Meiwes-Broer, ed. (Springer-Verlag, Heidelberg, 2000) 175-210; N. Agrait, A. Levy Yeyati, and J.M. van Ruitenbeek, to appear in Phys. Reports.

[2] G. Rubio, N. Agraït, and S. Viera, Phys. Rev. Lett. **76**, 2302 (1996).

[3] J.M. Krans, J.M. van Ruitenbeek, V.V. Fisun, I.K. Yanson, and L.J. de Jongh, Nature (London) **375**, 767 (1995).

[4] A.I. Yanson, Ph.D. thesis, University of Leiden, 2001.

[5] J.C. Cuevas, A.Levy Yeyati, and A. Martín-Rodero, Phys. Rev. Lett. **80**, 1066 (1998).

[6] A.P. Sutton and J.B. Pethica, J.Phys.: Cond. Mat. **2**, 5317 (1990); U. Landman, W.D. Luedtke, N.A. Burnham, and R. Colton, Science **248**, 454 (1990).

[7] O.Yu. Kolesnychenko, A.J. Toonen, O.I. Shklyarevskii, and H. van Kempen, Appl. Phys. Lett. **79**, 2707 (2001).

[8] A. Correia, M.I. Marqués, and N. García, J. Vac. Sci. Techn. B **15**, 548 (1997).

[9] G. Cross, A. Schirmeisen, A. Stalder, P. Grütter, M. Tschudy, and U. Dürig, Phys. Rev. Lett. **80** 4685 (1998).

[10] O.Yu. Kolesnychenko, O. I. Shklyarevskii, and H. van Kempen, Rev. Sci. Instrum. **70**, 1442 (1999).

[11] The integral $\int(|\partial_z G(z)|+\varepsilon)^{-1}dz$, where $\varepsilon>0$ is a small number used to prevent singularities, was calculated for each conductance trace within an interval $G(z)/G_0 \in [0.3, 3.3]$ and its value was used to select the curves with distinct plateaus.

[12] P.A. Taylor, J.S. Nelson, and B.W. Dodson, Phys. Rev. B **44**, 5834 (1991).

[13] J. Riedle, P. Gumbsch, and H.F. Fischmeister, Phys. Rev. Lett. **76** 3594 (1996).

[14] J.A. Torres, J.I. Pascual, and J.J. Saenz, Phys. Rev. B **49**, 16581 (1994).

[15] B. Ludoph, N. van der Post, E.N. Bratus, E.V. Bezuglyi, V.S. Shumeiko, G. Wendin, and J.M. van Ruitenbeek, Phys. Rev. B **61**, 8561 (2000).

[16] S. Ohnishi and M. Tsukuda, Solid State Commun. **71**, 391 (1989).

[17] C.J. Chen, Phys. Rev. B **42** 8841 (1990).

[18] M. Posternak, H. Krakauer, A.J. Freeman, and D.D. Koeling, Phys. Rev. B **21**, 5601 (1980).

[19] O.Yu. Kolesnychenko, Ph.D. thesis, University of Nijmegen, 2002.

[20] S.B. Legoas, A.A. Araujo, B. Laks, A.B. Klautau, and S. Frota-Pessôa, Phys. Rev. B **61**, 10417 (2000).